ВЫСОКОМОЛЕКУЛЯРНЫЕ СОЕДИНЕНИЯ, Серия А, 2011, том 53, № 2, с. 239–247

КОМПОЗИТЫ

УДК 541.64:547.915

PREPARATION OF POLYLACTIC ACID/EPOXIDIZED PALM OIL/FATTY NITROGEN COMPOUNDS MODIFIED CLAY NANOCOMPOSITES BY MELT BLENDING[1]

© 2011 г. Emad A. Jaffar Al-Mulla

Department of Chemistry, College of Science, University of Kufa, AnNajaf, Iraq

e-mail: emadaalmulla@yahoo.com

Received March 21, 2010
Revised Manuscript Received July 9, 2010

Abstract—In this study, new biopolymer nanocomposites have been prepared. Fatty nitrogen compounds (FNCs); fatty amide (FA), fatty hydroxamic acid (FHA), and carbonyl difatty amide (CDFA), which were synthesized from palm oil, have been used as one of organic compounds to modify natural clay (sodium montmorillonite). The clay modification was carried out by stirring the clay particles in an aqueous solution of FA, FHA, and CDFA by which the clay layer distance increases from 1.23 to 2.71, 2.91 and 3.23 nm, respectively. The modified clay was then used in the preparation of the polylactic acid/epoxidized palm oil (PLA/EPO) blend nanocomposites. The interaction of the modifier in the clay layer was characterized by X-ray diffraction (XRD), and Fourier transform infrared (FTIR). Elemental analysis was used to estimate the presence of FNCs in the clay. The nanocomposites were synthesized by melt blending of the modified clay and PLA/EPO blend at the weight ratio of 80/20. The nanocomposites were then characterized using XRD, transmission electron microscopy (TEM), thermogravimetric analysis (TGA), and tensile properties measurements. The XRD and TEM results confirmed the production of nanocomposites. PLA/EPO modified clay nanocomposites show higher thermal stability and significant improvement of mechanical properties in comparison with those of the PLA/EPO blend.

INTRODUCTION

Biodegradable polymers have recently much attracted in the scientific community due to a rapid growth of intensive interest in the global environment as alternative of petroleum-based polymeric materials.

One of the most promising candidates of biodegradable synthetic polymers is PLA [1]. PLA can be obtained from renewable resources by means of a fermentation process using sugar from corn either by ring-opening polymerization or by condensation polymerization. It is linear aliphatic thermoplastic polyester and is readily biodegradable by enzymatic way [2–4].

In addition to its application in textile industries, automotive and clinical uses, PLA represents a good candidate to produce disposable packaging due to its good mechanical properties and processability [5–7]. However, high tensile, high modulus, low elongation at break and high price limit its application. Therefore, the tailoring of its properties to reach end-users demands is required.

Attempts have been made to enhance the flexibility and other mechanical properties by blending of PLA with other polymers such as polycaprolactone, polybutylene succinate or polyetherurethane [8–11]. Low molecular weight plasticizers such as polyethylene glycol, polypropylene glycol and citrate esters were also used to improve of the thermal and mechanical properties of PLA [12–15].

The incorporation of organoclays in the polymer to produce nanocomposite is another mean to modify the property balance of a material. The improvements in thermal stability, physical and mechanical properties can be achieved by addition of 2–5 wt% of organoclays in comparison to the neat polymer [16–18].

The modifying natural clay (montmorillonite) may carried out via exchanging the original inter-layer cations by organic cations where transform from organophobic to organophilic materials and significantly increase the basal spacing of the clay layers [19]. It is generally accepted that the extent of swelling depends on the length of the alkyl chain and the cation exchange capacity of the clay [20]. Organoclays are mainly obtained by exchanging cations in the clay minerals which contain hydrated Na^+ ions with alkylamidonium [21].

Processing and properties of PLA/thermoplastic starch/montmorillonite nanocomposites were investigated and characterized using X-Ray diffraction, transmission electron microscopy and tensile measurements. The results show improvement in tensile modulus and strength and to a reduction in fracture toughness [22].

[1] Статья печатается в представленном авторами виде.

Table 1. The optimization of basal spacing of modified montmorillonite with different amounts of fatty nitrogen compounds and hydrochloric acid

Amount of FNCs (g) in 4.00 g of MMT	Conc. HCl, ml	d-spacing, nm		
		FA-MMT	FHA-MMT	CDFA-MMT
1.00	4.00	1.29	1.32	1.59
1.50	4.00	1.30	1.39	1.77
2.00	4.00	1.34	1.44	1.85
2.50	4.00	1.40	1.54	1.91
3.00	4.00	1.45	1.60	2.03
3.50	4.00	1.50	1.67	2.10
4.00	4.00	1.55	1.73	2.19
4.50	4.00	1.62	1.82	2.27
5.00	4.00	1.63	1.83	2.29
4.50	6.00	1.72	2.01	2.48
4.50	8.00	1.87	2.29	2.59
4.50	10.00	2.01	2.42	2.72
4.50	12.00	2.12	2.61	2.91
4.50	14.00	2.41	2.74	3.11
4.50	16.00	2.69	2.89	3.21
4.50	18.00	2.70	2.91	3.22

Plasticized PLA based nanocomposites were prepared and characterized with polyethyleneglycol and montmorillonite. It is reported that the organo-modified montmorillonites-based composites have shown the possible competition between the polymer matrix and the plasticizer for the intercalation between the alumino-silicates layers [23].

In this study, fatty nitrogen compounds (FNCs) synthesized from palm oil were used for modification of montmorillonite. The presence of long chains fatty acids (mainly 16 and 18 carbon atoms) in FNCs containing O and N donor set suggests FNCs should be very useful as surfactants for clay modification. The use of FNCs reduces the dependent on petroleum based surfactants. The present study show plasticized PLA based nanocomposites with epoxidized palm oil (EPO) and montmorillonite modified by DNCs. EPO is an epoxidized derivative of a mixture of esters of glycerol with various saturated and unsaturated fatty acids. It is important for many chemical industries as they are derived from renewable, biodegradable, environmental friendly and easily available raw materials.

EXPERIMENTAL

Materials

Epoxidized palm oil was provided by Advanced Oleochemical Technology Division (AOTD), Malaysia. Sodium montmorillonite (Kunipia F) was obtained from Kunimine Ind. Co. Japan. Polylactic acid and chloroform were purchases through local suppliers from T.J. Baker, USA and Merck, Germany, respectively.

Preparation of Organoclay

Organoclay was prepared by cationic exchange process where Na^+ in the montmorillonite was exchanged with alkylamidonium ion from FNCs synthesized from triacylglycerides, which were reported in our previous papers [24–26], in an aqueous solution. 4.00 g of sodium montmorillonite (Na-MMT) was stirred vigorously in 600 ml of hot distilled water for one hour to form a clay suspension. Subsequently, designated amount of fatty nitrogen compounds which had been dissolved in 400 ml of hot water and desired amount of concentrated acid hydrochloride (HCl) was added into the clay suspension of fatty nitrogen compounds. After stirred vigorously for one hour at 80°C, the organoclay suspension was filtered and washed with distilled water until no chloride was detected with 1.0 M silver nitrate solution. It was then dried at 60 °C for 72 hours. The dried organoclay was ground until the particle size was less than 100 μm before the preparation of nanocomposite. The amounts of hydrochloric acid, and FNCs used in this study were listed in Table 1.

Preparation of PLA/EPO–clay Nanocomposites

The designed amount of PLA/EPO ratio were prepared by an internal mixer (Haake Polydrive), using different conditions (temperature, speed and time) in order to obtain the optimum conditions which were 185°C, 50 rpm and 12 minutes, respectively. To prepare a sample of the composite, a specific amount of PLA was first melted and mixed thoroughly with appropriate amount of PCL for 2 minutes. Various amounts of organoclays (1, 2, 3, 4, and 5%) were incorporated into the blend in the third minute. The mixture was compressmoulded into sheet of 1 mm thickness sheets under a pressure of 100 kg cm^{-1} in a standard hot press at 150°C for 15 min, and cooled pressed process for 10 minutes to obtain a good blend film. The amount of PLA/EPO and the modified clay used in this study are listed in Table 2.

Characterization

X-Ray diffraction (XRD) analysis. X-ray Diffraction (XRD) study was carried out using Shimadzu XRD 6000 diffractometer with CuK radiation (λ = = 0.15406 nm). The diffractogram was scanned in the ranges from 2° to 10° at a scan rate of 1° min^{-1}.

Fourier transform infrared (FTIR) spectroscopy. The FTIR spectra of the samples were recorded by the FTIR spectrophotometer (Perkin Elmer FT-IR-Spectrum BX, USA) using KBr disc technique.

Elemental analysis. Elemental analyzer (LEO CHNS-932) was used for quantative analysis of nitrogen contents in the organoclay. The determination was carried out under N_2 atmospheric conditions using the sulfamethazine as a standard.

Thermogravimetric analysis (TGA). The thermal stability of the samples was studied by using Perkin Elmer model TGA 7 Thermogravimetry Analyzer. The samples were heated from 35 to 800°C with the heating rate of 10°C/min under nitrogen atmosphere with a nitrogen flow rate of 20 mL/min.

Transmission electron microscopy (TEM). The dispersion of clay was studied by using Energy Filtering Transmission Electron Microscopy (EFTEM). TEM pictures were taken in a LEO 912 AB Energy Filtering Transmission Electron Microscope with an acceleration voltage of 120 keV. The specimens were prepared using a Ultracut E (Reichert and Jung) cryomicrotome. Thin sections of about 100 nm were cut with a diamond knife at −120°C.

Tensile properties measurements. The tensile strength, tensile modulus and elongation at break were measured by using Instron Universal Testing Machine 4301 at 5 mm/min of crosshead speed in accordance to ASTMD638 [27]. Seven samples were used for the tensile test and an average of five results was taken as the resultant value.

RESULTS AND DISCUSSION

According to our recent paper [28], the PLA/EPO blend at the weight ratio of 80/20 has the highest elongation at break. Therefore, this ratio was used in the subsequent experiments.

Figure 1 shows the effect of clay content on the tensile properties of PLA/EPO/Na-MMT microcomposites, PLA/EPO/CDFA-MMT, PLA/EPO/FA-MMT, and PLA/EPO/FAH-MMT nanocomposites. The reinforcing effect of unmodified montmorillonite in the PLA/EPO matrix was increased with low rate of increment. The maximum tensile strength was obtained when the clay content was 2% weight. Further increase of clay content decreases tensile strength. Ma-MMT acts as conventional particulate filler in the PLA/EPO matrix. Low tensile strength is obtained for PLA/EPO/Na-MMT because the clay–clay interactions are stronger than that PLA/EPO-clay interactions [29]. A poor compatibility between the clay and PLA/EPO matrix is expected as the mixing is at micro level [30]. A similar behavior of the clay content effect on the modulus and elongation at break of PLA/EPO/Na-MMT is observed (Figs. 2 and 3).

Table 2. The amounts of PLA, EPO and modified clay in the nanocomposites

Sample Identity	Weight of PLA, g	Weight of EPO, g	Weight of Organo-clay, g
8PLA 2EPO	4.00	1.00	0.00
8PLA 2EPO mod1	3.96	0.99	0.05
8PLA 2EPO mod2	3.92	0.98	0.10
8PLA 2EPO mod3	3.88	0.97	0.15
8PLA 2EPO mod4	3.84	0.96	0.20
8PLA 2EPO mod5	3.80	0.95	0.25

Note. mod1, mod2, mod3, mod4 and mod5 = 1%, 2%, 3%, 4% and 5% weight of organoclay, respectively.

The increment of tensile strength, modulus, and elongation at break for the nanocomposites with FA-MMT, FHA-MMT, and CDFA-MMT loadings are similar to that of microcomposites. However, the rate of the increment of tensile properties for the nanocomposites increases.

The highest tensile strength, modulus, and elongation at break of the FA-MMT, FHA-MMT, and CDFA-MMT nanocomposites are obtained when

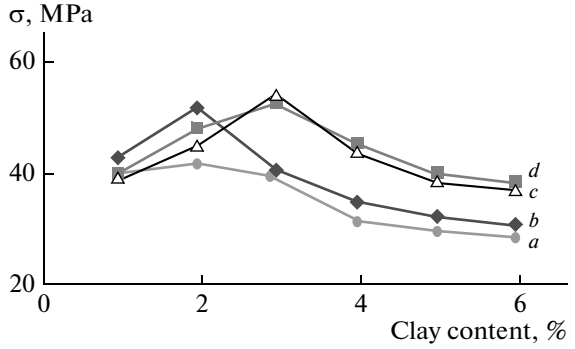

Fig. 1. Effect of clay content on the tensile strength σ of (*a*) PLA/EPO/Na-MMT, (*b*) PLA/EPO/CDFA-MMT, (*c*) PLA/EPO/FA-MMT, and (*d*) PLA/EPO/FHA-MMT nanocomposites.

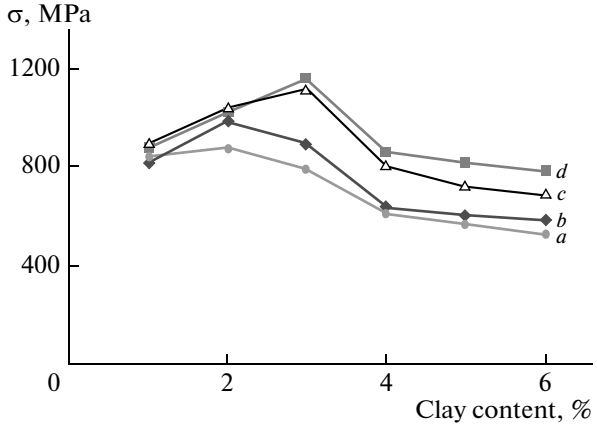

Fig. 2. Tensile modulus of (*a*) PLA/EPO/MMT, (*b*) PLA/EPO/CDFA-MMT, (*c*) PLA/EPO/FHA-MMT, and (*d*) PLA/EPO/FA-MMT nanocomposites.

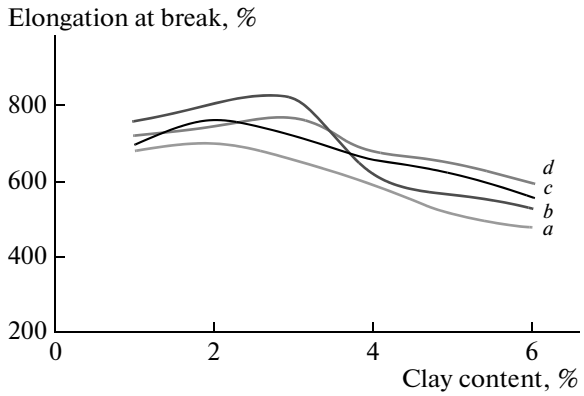

Fig. 3. Elangotion at break of (*a*) PLA/EPO/MMT, (*b*) PLA/EPO/FA-MMT, (*c*) PLA/EPO/CDFA-MMT, and (*d*) PLA/EPO/FHA-MMT nanocomposites.

3% of FA-MMT or FHA-MMT and 2% of CDFA-MMT loadings are used (Figs. 1–3). The enhancing effect of the FA-MMT, FHA-MMT, and CDFA-MMT on the mechanical properties is probably due to the increase of the amount of the incorporated PLA/EPO chains in the clay layers. The polymer–clay interactions include the interactions of the intercalated PLA/EPO chains with surface layers of the silicates. However, the tensile strength modulus, and elongation at break decrease when the FA-MMT, FHA-MMT, and CDFA-MMT loadings are increased to more than 2% and 3% of FA-MMT and FHA-MMT; and CDFA-MMT, respectively. The decrease of tensile strength, modulus, and elongation at break is due to the decrease of the PLA/EPO chains interact with the clay as the clay coagglomerates.

According to the Bragg's law ($n\lambda = 2d\sin\theta$), the d refers to the distance of two consecutive clay layers, λ is the wavelength of the intercept X-rays at the incident angle θ.

The presence of FNCs chain in the galleries makes the originally hydrophilic to organophilic silicate and thus increases the layer-to-layer spacing of Na-MMT [17]. By using X-ray diffraction, Na-MMT shows a d001 diffraction peak at $2\theta = 7.21°$ which assigns to the interlayer distance of the natural montmorillonite with a basal spacing of 1.23 nm. Na-MMT was surface treated with FNCs as intercalation agent through cation exchange process. The cationic head groups of the intercalation agent molecule would preferentially reside at the layer surface and the aliphatic tail will radiate a ways from the surface.

Table 3. Diffraction angle and basal spacing of natural clay (Na-MMT) and modified clays with the FA-MMT, FHA-MMT and CDFA-MMT

Sample	Exchanged Cation	2θ, degree	d-spacing, nm
Na-MMT	Na^+	7.21	1.23
FA-MMT	$RCO-N^+H_3$	3.27	2.71
FHA-MMT	$RCO-N^+H_2OH$	3.05	2.91
CDFA-MMT	$(RCO)_2\,NHCON^+H_2$	2.77	3.23

The optimum amount of FNCs and HCl to reach maximum d-spacing were studied. It was found that the maximum d-spacing was achieved when the amount of FNCs and HCl were 4.50 g and 16 ml, respectively (Table 1). It was observed no significant increase in d-spacing with further increase in FNCs and HCl. The maximum basal spacing of FA-MMT, FHA-MMT, and CDFA-MMT increases from 1.23 to 2.71, 2.91 and 3.23 nm, respectively (Table 3), indicating that these FNCs were successfully intercalated into the Na-MMT galleries (Fig. 4).

Greater basal spacing is observed for the CDFA-MMT than that of the FHA-MMT and FA-MMT, suggesting that CDFA adopts a paraffin arrangement in the silicate layer while a monolayer arrangement of FHA and FA molecules in the interlayer spacing of Na-MMT [31].

Figure 5 shows the XRD patterns of the nanocomposites prepared using of three different FNCs (alkylamidonium groups) modified montmorillonite nanocomposites. In the nanocomposites where the montmorillonite surface is pretreated with FA and FHA, the basal spacing of the clay increase to 3.13 and 3.31 nm, respectively. However, when the montmorillonite surface is pretreated with CDFA which has two fatty acids chains, the basal spacing further increases to 3.60 nm (Table 4). This is clearly shows that the basal spacing of organoclay in the polymer matrix increases with the increase of the size of the surfactant as it is observed by Agag and Takeichi [32]. These XRD patterns also suggest that all the nanocomposites produced are intercalated compounds.

The FTIR spectra of Na-MMT, FA-MMT, FHA-MMT, and CDFA-MMT are shown in Fig. 6. In the spectra of Na-MMT, the peaks at 3511, 1626 and 1009 cm^{-1} are due to the O–H stretching, interlayer water deformation and the Si–O stretching vibration, respectively. The other strong bands absorption at 510 cm^{-1} and 439 cm^{-1} indicate the presence of Al–O stretching and Si–O bending, respectively in the clay. The FA-MMT, FHA-MMT, and CDFA-MMT spectra show the major bands of FA, FHA, and CDFA spectra [24–26] in addition to the bands of the original Na-MMT. The band at around 1470 cm^{-1} suggests the existence of the ammonium ion. Therefore, these indicate that the FA, FHA, and CDFA were intercalated in the silicate layers.

Elemental analysis was used to estimate the amount of FA, FHA, and CDFA being intercalated into the clay galleries. Table 5 shows the results of N analyses of the FA, FHA, and CDFA and the mixtures of FA, FHA, and CDFA modified clay. The calculation is based on either atom carbon or atom nitrogen

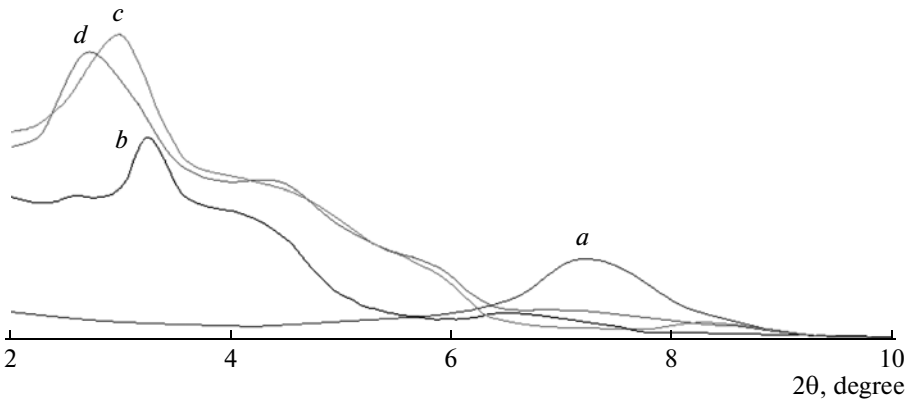

Fig. 4. XRD patterns of (*a*) Na-MMT, (*b*) FA-MMT, (*c*) FHA-MMT and (*d*) CDFA-MMT.

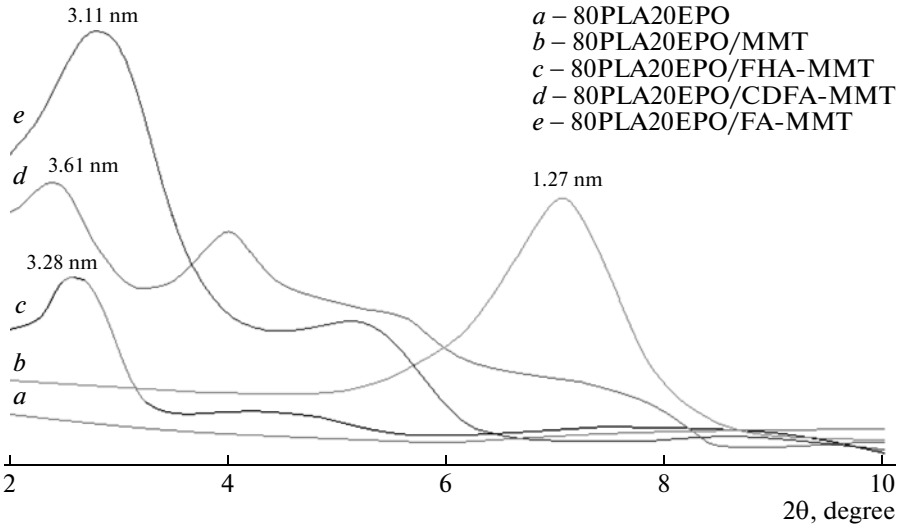

Fig. 5. XRD patterns of PLA/EPO/FNCs modified clay nanocomposites.

because if the increase of their content is only due to the presence of the organic molecule, the calculation does not base on the hydrogen content as there are possibilities of water molecules tapped between the layers of the unmodified clay. The high contents of N in all samples indicate that alkylamidonium cations were successfully exchanged into the clay. However, the %N in the unmodified clay is only 0.21%. The maximum amount of alkylamidonium cations adsorbed was almost equivalent to the cation exchange capacity of the clay indicating that the Na^+ in the clay can be easily replaced by the alkylamidonium cations. The amounts of FNCs present in the organoclay were calculated by the following equation:

$$\text{Amount of FNCs (mole)} = S/(100An),$$

where S is percentage of the N in the organoclay percentage of the N in the Na-MMT, A is atomic mass of N and n is number of N in the FNCs molecule.

Most of thermoanalytical studies reveal new insights into the structure of intercalated clays [33]. Thermogravimetric analysis (TGA) gives information on the structure of the intercalating molecules by the weight loss steps. Thermal degradation of MMT shows two steps [34]. The first one is before 200°C because of the volatilization of water sorbed on the external sur-

Table 4. Diffraction angle and basal spacing of PLA/EPO/FNCs modified clay nanocomposites

Sample	2θ, degree	d-spacing, nm
80PLA20EPO	0.00	0.00
80PLA20EPO/MMT	6.90	1.29
80PLA20EPO/FA-MMT	2.79	3.13
80PLA20EPO/FHA-MMT	2.64	3.31
80PLA20EPO/CDFA-MMT	2.41	3.60

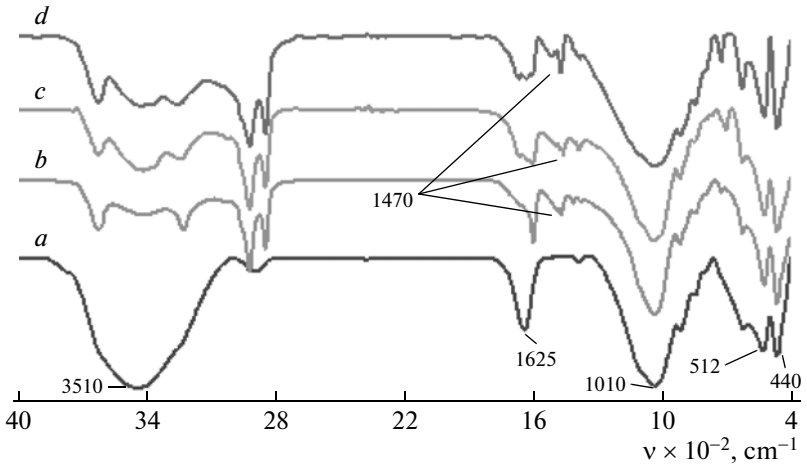

Fig. 6. FTIR spectra of (*a*) Na-MMT, (*b*) FA-MMT, (*c*) FHA-MMT, and (*d*) CDFA-MMT.

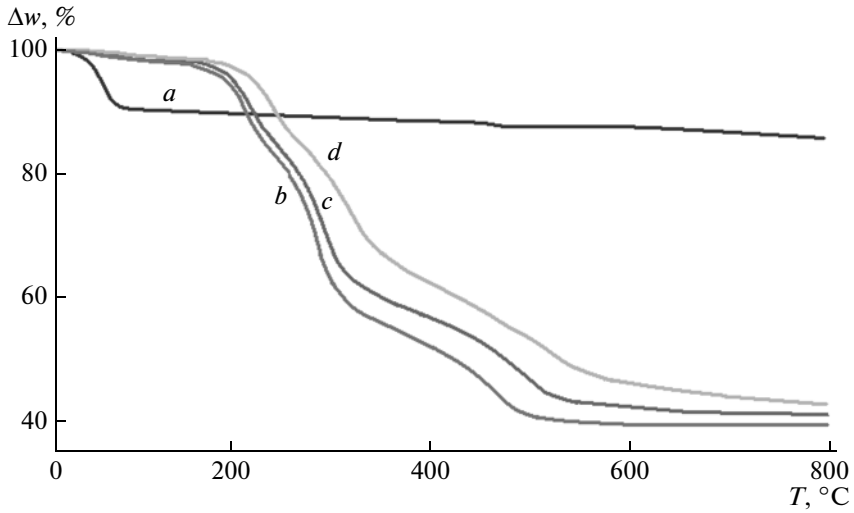

Fig. 7. DTG thermograms of (*a*) MMT, (b) FA-MMT, (*c*) FHA-MMT, and (*d*) CDFA-MMT.

faces of the MMT and water inside the interlayer space. The second step is in the range 500–1000°C due to the loss of hydroxyl groups of the MMT structure. The thermal degradation of the modified MMT can be explained in four steps. The first step occurs at below 200°C due to the vaporization of water. Decomposition of surfactant takes place in the second step between 200–500°C. Dehydroxylation of the aluminosilicates at the temperature range of 500–800°C happens in third step. In last step, the organic carbon reacts with inorganic oxygen (combustion reaction) at about 800°C.

Table 5. The amounts of N and alkylamidonium cations of FA, FHA and CDFA presence in the clay layers

Alkylamidonium cations modified clay	%N	mmol of alkylamidonium cations/1 g clay based on atom N
FA^+	2.50	1.78
FHA^+	2.69	1.92
$CDFA^+$	5.65	2.02

The weight loss curves (TGA) of the MMT, FA-MMT, FHA-MMT, and CDFA-MMT were illustrated in Fig. 7. MMT contains water due to hydrated sodium (Na^+) cations intercalated inside the clay layers. The presence of alkylamidonium groups within the MMT interlayer spacing lowers the surface energy of the inorganic structure and will transform organophobic to organophilic materials. The major difference between the thermogram of the unmodified clay and that of the organoclay is that the organic constituents in the organoclay decompose in the range of 200 to 500°C, as the organic constituent in the organoclay decomposes in this range. Figure 8 shows that the FA

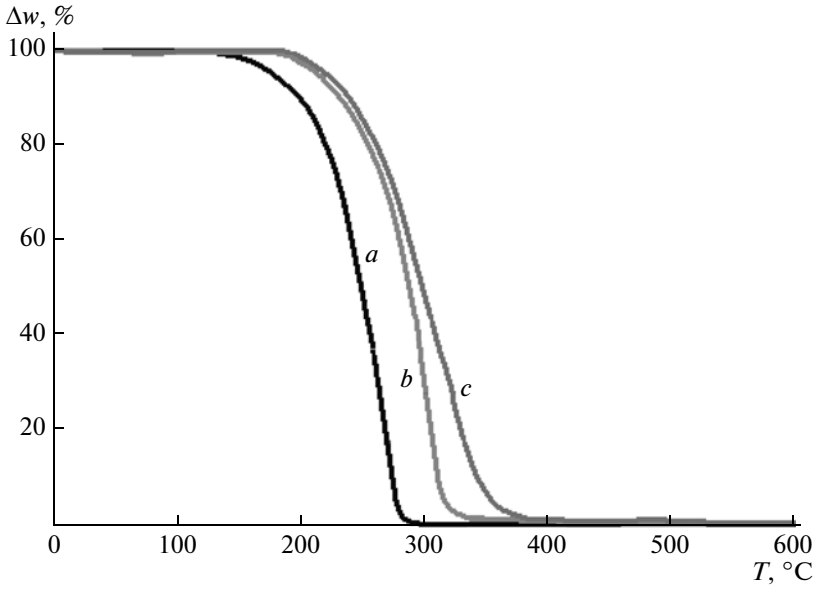

Fig. 8. TGA thermograms of (*a*) FA, (*b*) FHA, and (*c*) CDFA.

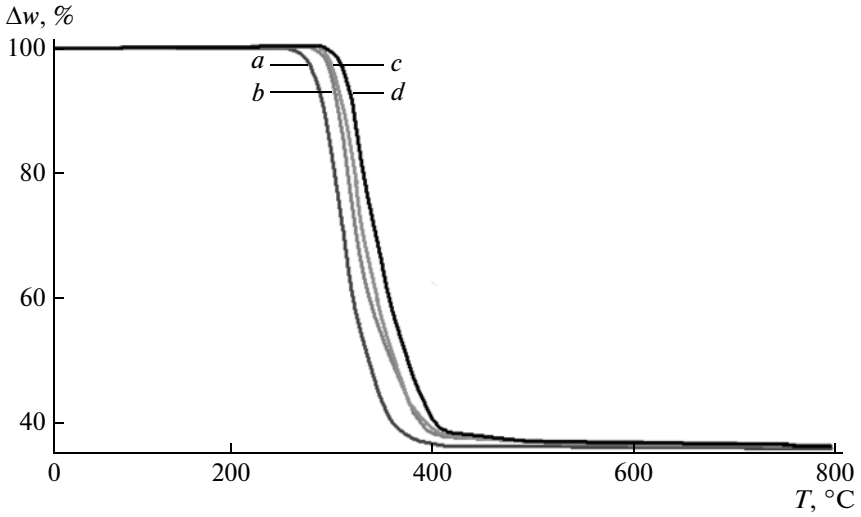

Fig. 9. TGA thermograms of (*a*) PLA/EPO blends, (*b*) PLA/EPO/FA-MMT, (*c*) PLA/EPO/FHA-MMT, and (*d*) PLA/EPO/CDFA-MMT nanocomposites.

decomposed as the temperature increased from 155 to 600°C. The decomposition process ended at 311°C. The FHA started decomposing at higher temperatures than that of the FA which started at 190°C and ended at 354°C. CDFA had the highest decomposition temperature (started at 194°C and ended at 399°C). It can be observed that the decomposition temperatures of the FA-MMT, FHA-MMT and CDFA-MMT were higher than those of the pure of FA, FHA, and CDFA. The increase in the decomposition temperatures of these FNCs in the organoclays implies that there is a strong intermolecular interaction between the alkylamidonium cations and the clay. In other words, after the ion exchange the FNCs is intercalated and attached to silicate layers of the clay and hence their decomposition temperatures increase.

Thermogravimetric analyses were done on PLA/EPO/FNCs-MMT nanocomposites in order to determine the effect of modified clay content in the polymer matrix on thermal properties. The results of TGA are shown in Fig. 9. The onset of the degradation of the nanocomposites is higher, that is 281, 287, and 293°C, for PLA/EPO containing FA-MMT, FHA-MMT, and CDFA-MMT, respectively, compared to the PLA/EPO blend (269°C). The results show that the thermal stability increases with adding the FNCs.

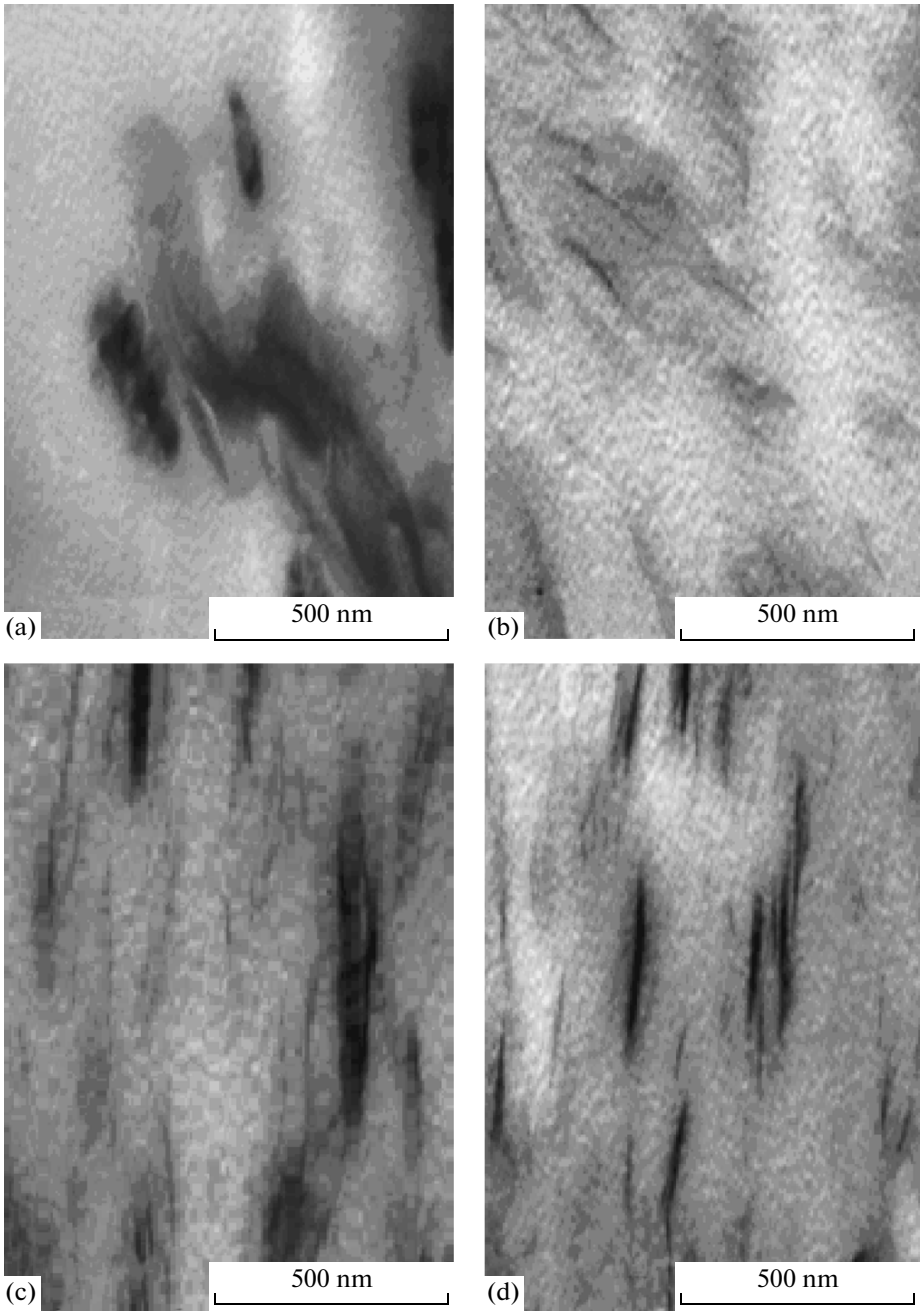

Fig. 10. TEM micrographs of (a) PLA/EPO Na-MMT, (b) PLA/EPO/CDFA-MMT, (c) PLA/EPO/FA-MMT, and (d) PLA/EPO/FHA-MMT composites.

The presence of silicate layers dispersed homogeneously in polymer sheet hinders the permeability of volatile degradation products out from the material and helps delay the degradation of the nanocomposites [35].

Figures 10a, b, c, and d show transmission electron microscopy (TEM) micrographs of the PLA/EPO composites reinforced with Na-MMT, CDFA-MMT, FHA-MMT, and FA-MMT, respectively. From the PLA/EPO/Na-MMT micrograph, it can be observed that the original Na-MMT stack morphology was fully preserved with PLA/EPO due to the incompatible nature of both constituents (Fig. 10a). Dark bundles represent the thickness of the individual clay layers or agglomerates. Figures 10b and c exhibit the TEM images of PLA/EPO/3% FA-MMT, and PLA/EPO/3% FHA-MMT nanocomposites, which show a good properties and composite effect. The dark bundles of modified clay are dispersed in PLA/EPO blend with intercalated state, which can be observed clearly in the images. The TEM micrograph of

PLA/EPO/2% CDFA-MMT (Fig. 10b) shows a higher degree of intercalation and some exfoliated zones.

CONCLUSIONS

Organophilic montmorillonites (FA-MMT, FHA-MMT, and CDFA-MMT) were successfully prepared by cation exchange process. FTIR spectra indicate that the presence of alkylamidonium group resulting from the modification. The basal spacing (001 d) of FA-MMT, FHA-MMT, and CDFA-MMT increases from 1.23 to 2.71, 2.91 and 3.23 nm, respectively. Thermogravimetric analysis shows that the decomposition temperature of FA, FHA, and CDFA in the organoclay is higher compared with that of the pure of these fatty nitrogen compounds, suggesting that there is a strong intermolecular interaction between the alkylamidonium and the montmorillonite. PLA/EPO clay nanocomposites have been prepared by incorporating of 2% CDFA-MMT and 3% of both FA-MMT and FHA-MMT. TEM analysis shows that the prepared nanocomposites were an intercalated (FA-MMT and FHA-MMT) and partially exfoliated types (CDFA-MMT). The TGA thermograms of PLA/EPO/clay nanocomposites demonstrate higher decomposition temperatures in comparison with that of PLA/EPO composites. The XRD patterns revealed that the interlayer distance of organoclays in PLA/EPO blend was significantly increased.

REFERENCES

1. Y. Lemmouchi, M. Murariu, A. Santos, A. Schacht, and P. Dubois, Eur. Polym. J. **45**, 2839 (2009).
2. H. Tsuji and Y. Ikada, J. Appl. Polym. Sci. **67**, 405 (1998).
3. T. Iwata and Y. Doi, Macromolecules **31**, 2461 (1998).
4. D. Sawai, K. Takahashi, T. Imamura, K. Nakamura, T. Kanamoto, and S. Hyon, Polym. Sci. Polym. Phys. **40**, 95 (2002).
5. M. Murariu, A. Ferreira, M. Pluta, L. Bonnaud, M. Alexandre, and P. Duboi, Eur. Polym. J. **44**, 3842 (2008).
6. R. Auras, S. Singh, and J. Singh, Packag. Technol. Sci. **18**, 207 (2005).
7. R. Auras, B. Harte, S. Selke, and R. Hernandez, J. Plastic. Film. Sheet. **19**, 123 (2003).
8. A. Nijenhuis, E. Colstee, D. Grijpma, and A. Pennings, Polymer **37**, 5849 (1996).
9. L. Liu, S. Li, H. Garreau, and M. Vert, Biomacromol **1**, 350 (2000).
10. N. Lopez-Rodriguez, A. Lopez-Arraiza, E. Meaurio, and J. Sarasua, Polym. Eng. Sci. **46**, 1299 (2006).
11. Y. Li and H. Shimizu, Macromol. Biosci. **7**, 921 (2007).
12. M. Baiardo, G. Frisoni, M. Scandola, M. Rimelen, D. Lips, K. Ruffieux, and E. Wintermantel, J. Appl. Polym. Sci. **90**, 1731 (2003).
13. N. Ogata, H. Sasayama, K. Nakane, and T. Ogihara, J. Appl. Polym. Sci. **89**, 474 (2003).
14. Z. Kulinski and E. Piorkowska, Polymer **46**, 10290 (2005).
15. Z. Ren, L. Dong, and Y. Yang, J. Appl. Polym. Sci. **101**, 1583 (2006).
16. P. LeBaron, Z. Wang, and T. Pinnavaia, Appl. Clay. Sci. **15**, 11 (1999).
17. M. Alexandre and P. Dubois, Mater. Sci. Eng. R. Rep. **28**, 1 (2000).
18. A. Okada and A. Usuki, Macromol. Mater. Eng. **291**, 1449 (2006).
19. E. Giannelis, Adv. Mater. **8**, 29 (1996).
20. B. Zidelkheir1, and M. Abdelgoad, J. Therm. Anal. Cal. **94**, 181 (2008).
21. A. Pérez-Santano, R. Trujillano, C. Belver, A. Gil, and M. Vicente, J. Colloid. Interface. Sci. **284**, 239 (2005).
22. O. Arroyo, M. Huneault, B. Favis, and M. Bureau, Polym. Compos. **31**, 114 (2010).
23. M. Paul, M. Alexandre, P. Degée, C. Henrist, A. Rulmont, and P. Dubois, Polymer **44**, 443 (2003).
24. E. Al-Mulla, W. Yunus, N. Ibrahim, and M. Rahman, J. Oleo Sci. **58**, 467 (2009).
25. W. Hoidy, M. Ahmad, E. Al-Mulla, W. Yunus, and N. Ibrahim, J. Oleo Sci. **59**, 15 (2010).
26. E. Al-Mulla, W. Yunus, N. Ibrahim, and M. Rahman, J. Oleo Sci. **59**, 80 (2010).
27. ASTM D638-03, Standard test method for tensile properties of plastics (2004).
28. E. Al-Mulla, W. Yunus, N. Ibrahim, and M. Rahman, J. Mater. Sci. **45**, 1942 (2010).
29. Y. Vu, J. Mark, L. Pham, and M. Engelhardt, J. Appl. Polym. Sci. **82**, 1391 (2001).
30. M. Arroyo, M. Lopez-Manchado, and B. Herrero, Polymer **44**, 2447 (2003).
31. M. Pospisil, A. Kalcndova, P. Capkova, J. Simonik, and M. Valaskova, J. Colloid. Interface Sci. **227**, 154 (2004).
32. T. Agag and T. Takeichi, Polymer **41**, 7083 (2000).
33. Y. Xi Y, W. Martens, H. He, and R. Frost, J. Therm. Anal. Cal. **81**, 91 (2005).
34. M. Manchado and B. Herrero, Polymer **44**, 2447 (2003).
35. S. Jamaliah, M. Wan, Z. Khairul, M. Dahlan, and A. Mansor, Polym. Test **24**, 211 (2005).